PAP file

United States Department of the Interior
Bureau of Reclamation
Engineering and Research Center

Translation No.
Team No. General
Book No. 12,672
Paper No.

XXXXXXXXXXXXXXXXXXXXXXXXXXXXXXXXXXXXXXXXXXXXXXXXXXXXXXXXXXXXXXXXXXXXXXXXXXXX

EFFECTS OF AERATION ON FLOW FIELD PRESSURE

by

Huang Jianbo

Dalian Engineering College

Translated from the Chinese: Journal of Hydraulic Engineering,
Beijing, No. 5, pp. 43-46, 1987

Translated by Dr. David Hsu, Foreign Resources Associates

XXXXXXXXXXXXXXXXXXXXXXXXXXXXXXXXXXXXXXXXXXXXXXXXXXXXXXXXXXXXXXXXXXXXXXXXXXXXXX

Division of Foreign Activities
Code D-2000

USBR Translations
Denver, Colorado
January 1988

Team No. General
Book No. 12,672

EFFECTS OF AERATION ON FLOW FIELD PRESSURE

by

Huang Jianbo

I. INTRODUCTION

A common practice in hydraulic engineering for preventing cavitation erosion is to aerate the flow along a solid boundary. Although this method is widely used and often produces satisfactory results, research shows that aeration is not always desirable. Basically, aeration has the following three effects: (1) It affects the pressure in the flow. Both theory and experiment show that aeration of a low-pressure zone in a flow increases the pressure substantially. This problem shall be analyzed here. (2) It affects the distribution of the gas nuclei in the water and increases the number of large gas nuclei. (3) It affects the extinction pressure of the gas bubbles. This problem has been studied before [2], and the analysis shows that only moderate aeration is needed to lower the extinction pressure of the gas bubbles.

In this work, theoretical analysis is first conducted for the effects of air entrainment on the pressure in a water flow; then, experimental comparisons are made for the pressure distribution of a flow around a bow segment with and without air entrainment.

II. THEORETICAL ANALYSIS

When the low-pressure zone of a water flow is aerated the air expands in the flow and does work against the flow, thereby increasing the flow's energy. Let the rate of water flow through the aerated zone be Q, the rate of air flow through any cross-section (e.g., section 2 in Figure 1) be αQ,

and the rate of air flow at the aeration point be $\alpha_0 Q$. Then the difference between the energy flux through section 2 and through section 1 per unit time is the work done by the entrained air in a unit time. The energy equation therefore can be written as

$$Q_m(p_m+\rho_m V_m^2/2)-Q(p+\rho V^2/2)=J, \tag{1}$$

where m represents a mixture of gas and liquid, and p, V, and ρ are respectively the pressure, flow velocity and density. Quantities without a subscript pertain to the liquid, and J is the work done by the expanding air in a unit time.

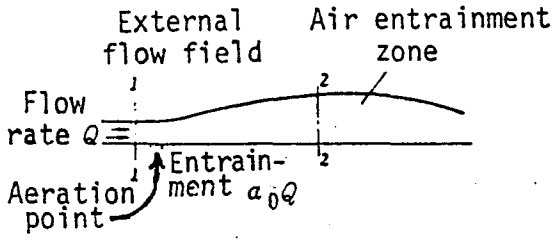

Figure 1. Air entrainment in the low-pressure zone.

Assuming the expansion of the air is an isothermal process of an ideal gas, we have

$$J=\alpha_0 Q p_{g0}\ln(p/p_g)=\alpha_0 Q p_{g0}\ln(\Omega_g/\Omega_{g0}), \tag{2}$$

where subscript g indicates quantities of the gas, Ω is volume, and subscript 0 represents the initial condition (state at the aeration point). There is no air entrainment before section 1, and the Bernoulli equation for a liquid applies:

$$p+\rho V^2/2=p_\infty+\rho V_\infty^2/2, \tag{3}$$

Here the subscript ∞ represents free flow. Since $Q_m=(1+\alpha)Q$ and $\rho_m\approx(1-\alpha)\rho$, the effect of the entrained air on the water flow velocity is quite small. (The air density is very low and its impedance against flow is negligible.) Thus, $V_m\approx V$ and (1) can be rewritten as

$$p_m(1+\alpha)-\rho\alpha^2 V/2=p+\alpha_0 p_{g0}\ln(\Omega_g/\Omega_{g0}). \tag{4}$$

Table 1

C_p	$p(10^5 P_a)$	$\alpha_0 = 0.01$				$\alpha_0 = 0.05$			
		ξ	α	p_m	C_{pm}	ξ	α	p_m	C_{pm}
-1.2	-0.449	2.81	0.223	0.074	-0.767	1.96	0.374	0.160	-0.695
-1.1	-0.328	2.72	0.201	0.078	-0.763	1.91	0.347	0.170	-0.687
-1.0	-0.208	2.59	0.174	0.086	-0.757	1.84	0.313	0.186	-0.674
-0.9	-0.087	2.41	0.140	0.099	-0.746	1.77	0.276	0.207	-0.657
-0.8	0.034	2.16	0.100	0.127	-0.723	1.67	0.234	0.239	-0.630
-0.7	0.155	1.83	0.061	0.189	-0.672	1.57	0.193	0.284	-0.593
-0.6	0.276	1.56	0.038	0.289	-0.589	1.46	0.155	0.347	-0.541
-0.5	0.396	1.38	0.026	0.400	-0.497	1.35	0.124	0.428	-0.474
-0.4	0.516	1.27	0.021	0.516	-0.401	1.26	0.100	0.525	-0.394
-0.3	0.638	1.18	0.016	0.633	-0.304	1.18	0.083	0.627	-0.309

Strictly speaking, one must calculate the growth of the bubble in the low-pressure zone in order to determine the ratio Ω_g/Ω_{g0}; however, before the bubble growth reaches the unstable state, its radius may still be determined from the equilibrium condition [3]:

$$p_m + 2S/R = p_v + p_{g_0}(R_0/R)^3, \tag{5}$$

where S is the surface tension of water, R is bubble radius, and p_v is the saturation vapor pressure of water. Let $\overline{R}_0$ be the average initial bubble radius and ξ be the growth factor ($\xi = \overline{R}/\overline{R}_0$) of the bubble at any location; then, $\alpha \approx \alpha_0 \xi^3$ and $\Omega_g/\Omega_{g0} \approx \xi^3$. Equations (4) and (5) can then be written as

$$p_m(1+\alpha_0\xi^3) - p_\infty - 3\alpha_0 p_{g_0} \ln\xi = (p_\infty - p_v)[\xi^3\alpha_0^{\frac{1}{2}}(1-C_p) + C_p]/\sigma, \tag{6}$$

$$p_m = p_v - 2S/\overline{R}_0\xi + p_{g_0}/\xi^3, \tag{7}$$

where $C_p = 2(p-p_\infty)/\rho V_\infty^2$, $\sigma = 2(p_\infty - p_v)/\rho V_\infty^2$.

We define C_{pm} as the pressure coefficient of the gas-liquid mixture, given by $C_{pm} = 2(p_m - p_\infty)/\rho V_\infty^2$. We also take $p_{g0} = 10^5 N/m^2$, $p_\infty = 10^5 N/m^2$, $p_v = 2500 N/m^2$, $\overline{R}_0 = 10^{-4} m$, $S = 0.0747 N/m$, and $\sigma = 0.8$. We then calculated the average

growth factor of the entrained air bubble and the average air-to-water volume ratio α, the pressure p_m and pressure coefficient C_{pm} of the mixture across the cross-section of the aerated region for different pressures p. The results are shown in Table 1. It can be seen from the data in Table 1 that (1) air entrainment has a pronounced effect on the average pressure of the water flow, (2) the lower the pressure the greater the air bubble average growth factor and hence the average air/water volume ratio α in a cross-sectional plane of constant α_0; and (3) with other flow conditions unchanged, the greater the air entrainment the higher the pressure in the water flow.

It should be pointed out that the above calculation of the average growth factor ξ of the air bubble is based on the equilibrium equation. This calculation is valid only when the computed ξ is less than the critical growth factor ξ_{cr}, of an unstable bubble. When the computed ξ is greater than ξ_{cr}, it implies that the air entrainment under the given flow conditions and air content can also lead to cavitation. From the equilibrium theory of a stable bubble [4] and the ideal gas equation of state of an isothermal process, we arrive at $p_{g0} = NT/R_0^3$ and $\xi_{cr} = \sqrt{3p_{g0}R_0/2S}$. (See page 50 of [4] for the meaning of the notations.) Take $p_{g0} = 10^5 \text{N/m}^2$, $R_0 = 10^{-4}$, and $S = 0.0747$ N/m, we have $\xi_{cr} \approx 14$. The bubble growth factor in the above calculation is therefore below the critical value.

III. EXPERIMENTAL ANALYSIS

In order to observe the effects of air entrainment on the pressure of the flow field, we performed tests of pressure distribution in a flow around a bow-shaped body with and without air entrainment. The tests were carried out in a rectangular water bath of 8 cm x 7 cm cross-section. The flow was controlled by a valve at the front end of the tank. The pressure in the flow

upstream from the bow-shaped body is made to be less than one atmosphere. The flow is aerated liberally via an aeration hole on the bottom of the tank and the air flow flux is determined by a rotor flow gauge. In our experiments the bow-shaped body had $L = 10$ cm and $\Delta = 1$, 1.67 cm. For the Δ=1.67 cm body, the aeration is done under strong cavitation conditions. It is observed that the bubble collapsing noise and the associated water vibration in the tank are greatly reduced after air entrainment. The time-averaged pressure of the aerated region is much higher. The observations also show that the periodic vibrations in the cavitation region near the tail of the bow-shaped body (caused mainly by the collapsing of bubbles due to the pulsating pressure) have been greatly reduced. The region near the tail becomes a zone of air and water mixture with a fairly constant spatial extent.

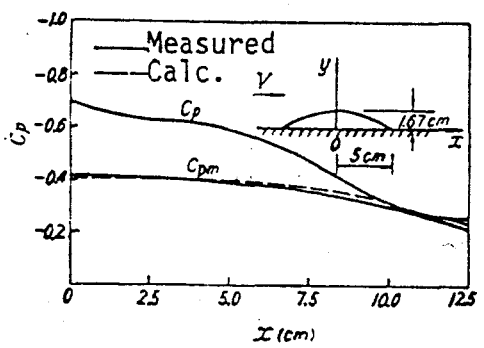

Figure 2. Comparison of measured and calculated C_{pm} of a bow-shaped body.

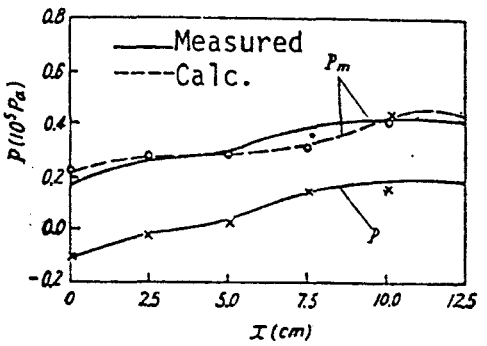

Figure 3. Comparison of measured and calculated p_m of a bow-shaped body.

Figures 2 and 3 show respectively the pressure coefficient and the fluid pressure of the $\Delta = 1.67$ cm body both with and without air entrainment. Also given are the computed results. The figures show excellent agreement between the measured and calculated quantities. The simple method for estimating

the effects of air entrainment on the average liquid pressure presented here is therefore feasible.

Figure 4 shows the measured and computed pressure coefficient before and after air entrainment for a $\Delta = 1$ cm bow-shaped body. The agreement is again satisfactory. For this body, the cavitation inception state has not been reached.

IV. EFFECTS OF AIR ENTRAINMENT ON CAVITATION

As shown above, air entrainment increases the pressure of the low-pressure zone in a water flow; it therefore has a suppressive effect on cavitation. On the other hand, air entrainment substantially increases the amount of gaseous nuclei in the flow and hence reduces the tensile strength of water. Whether air entrainment suppresses or promotes cavitation depends on which of the above two effects dominates. One view is that air entrainment always makes cavitation occur earlier. This is not always true. The onset of cavitation requires two simultaneous conditions: first, there must be an abundant supply of gas nuclei in the flow and, second, the pressure in the flow field must drop below the critical pressure so that the gas nuclei become unstable. Although air entrainment increases the supply of gas nuclei, it also changes the pressure in the flow field. With the proper amount of air entrainment, the pressure in the flow rises above the critical pressure for instability of the entrained air bubbles, the pressure is naturally higher than the instability critical pressure for smaller gas nuclei, and the second condition for cavitation is thus destroyed.

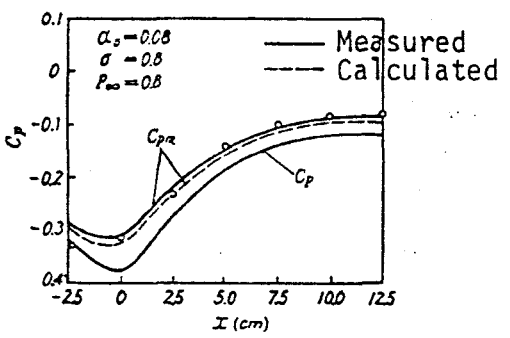

Figure 4. Measured and calculated C_{pm} of a bow-shaped body.

Due to limited experimental data, a quantitative estimate of the effects of air entrainment on the distribution of gas nuclei cannot be made at the present time.

Finally, it should be noted that the entrained air bubbles also can grow in the low-pressure zone of the flow field. However, as long as the growth factor is less than the critical instability growth factor for the bubbles, the growth will be stable and the physical process is totally different from the explosive growth of an unstable gas nucleus. This kind of growth cannot be regarded as cavitation.

REFERENCES

1. Oba R., Ito Y. Effects of flowing down bubbles on cavitation in a venturi. Rept. Inst. High-Speed Mech., Tohoku Univ., Vol. 44, pp. 1-14, 1981.
2. Huang Jianbo, Li Shihau, Ni Hangen. Effects of air entrainment on bubble collapse pressure. Journal of Hydraulic Engineering, No. 4, 1985.
3. Ni Hangen, Huang Jianbo, Xu Fusheng. Probabilistic estimate of cavitation inception number in a flow around a body. Journal of Hydraulic Engineering, No. 10, 1986.
4. Knapp *et al.* Cavitation and Cavitation Erosion. Translated by the Institute of Hydraulic Engineering and Hydroelectric Power. Published by the Water Resources and Electric Power Press, 1981.
5. Ni Hangen, Xu Fuseng, Huang Jianbo. On the impact pressure induced by collapsing bubbles. Proc. ISC, Sendai, Japan, 1986.